Experimental Evidence of Short Light Pulse Amplification Using Strong-Coupling Stimulated Brillouin Scattering in the Pump Depletion Regime

L. Lancia,[1,2] J.-R. Marquès,[1] M. Nakatsutsumi,[1] C. Riconda,[3] S. Weber,[4] S. Hüller,[5] A. Mančić,[1] P. Antici,[1,2] V. T. Tikhonchuk,[4] A. Héron,[5] P. Audebert,[1] and J. Fuchs[1,*]

[1]*LULI, École Polytechnique - CNRS - CEA, Université Paris 6, 91128 Palaiseau, France*
[2]*Dipartimento di Energetica, Università di Roma "La Sapienza," Via Scarpa 14-16, 00161 Roma, Italy*
[3]*LULI, Université Paris 6, École Polytechnique - CNRS - CEA, 75252 Paris, France*
[4]*Centre Lasers Intenses et Applications, CNRS, Université Bordeaux 1, CEA, 33405 Talence, France*
[5]*Centre de Physique Théorique, École Polytechnique - CNRS, 91128 Palaiseau, France*

(Received 9 June 2009; published 11 January 2010)

The energy transfer from a long (3.5 ps) pump pulse to a short (400 fs) seed pulse due to stimulated Brillouin backscattering in the strong-coupling regime is investigated. The two pulses, both at the same wavelength of 1.057 μm are quasicounterpropagating in a preformed underdense plasma. Relative amplification factors for the seed pulse of up to 32 are obtained. The maximum obtained amplified energy is 60 mJ. Simulations are in agreement with the experimental results and suggest paths for further improvement of the amplification scheme.

DOI: 10.1103/PhysRevLett.104.025001 PACS numbers: 52.38.Kd, 41.85.Ew, 52.38.Dx, 52.65.Rr

Interaction of short laser pulses in a plasma opens new possibilities for their amplification and manipulation [1–3]. Light amplification in plasma is based on an unidirectional energy transfer between a pump pulse and a shorter seed pulse in the presence of either an electron plasma wave (stimulated Raman scattering, SRS) [1,4] or an ion-acoustic wave (stimulated Brillouin scattering, SBS) [2]. Experimentally, and, in particular, with respect to short laser pulses, the energy transfer and amplification were demonstrated [5] in the regime corresponding to SRS excitation. Amplification of light pulses using SBS was abandoned since it is not suitable for pulses shorter than a few tens of ps due to the inherent limitation of the characteristic ion-acoustic plasma period $\sim\lambda_0/c_s$, where λ_0 is the laser wavelength and $c_s = (ZT_e/m_i)^{1/2}$ is the ion-acoustic velocity.

Interesting features of resonant coupling to plasma waves and energy transfer to another electromagnetic wave were predicted for the conditions where the laser plasma interaction occurs in the strong-coupling SBS regime (sc-SBS) [6,7]. This regime is characterized by low plasma temperatures (a few hundreds of eV) and high laser intensities. In this regime, the characteristic time scale of the plasma response is much shorter than λ_0/c_s, thus enabling energy transfer to short light pulses. The excited ion plasma wave is not an eigenmode, but a driven dynamic gratinglike perturbation. Thus, as suggested by numerical simulations [6], the electromagnetic coupling responsible for the short pulse amplification should be robust with respect to frequency mismatches and inhomogeneities of plasma density and temperature, contrary to the amplification schemes based on SRS [4].

In this Letter, we report the first experimental demonstration of short light pulse amplification using sc-SBS. Relative amplification factors of up to 32 for the transmitted seed pulse were obtained by crossing temporally coincident pulses with identical polarization in an Argon plasma with a density of $0.1n_c$. Systematic tests performed with 90° polarizations showed no amplification, ruling out any enhancement of the seed induced by effects others than electromagnetic coupling. The results are complemented by 1D hydrodynamic, 2D particle-in-cell (PIC) and 2D wave propagation simulations that allow insight into the physical mechanisms at play.

The experiment was carried out at the LULI 100 TW laser facility. Figure 1 shows the experimental setup [8]. The frequency chirped laser pulse (energy of 35 J, duration of 400 ps full width at half maximum, FWHM, wavelength $\lambda_o = 1.057$ μm, bandwidth of 6 nm FWHM) was split into three pulses: an ionization beam of 30 J, a pump beam of $E_{\text{pump}} = 2$ J, and a seed beam of $\sim$15 mJ. These three

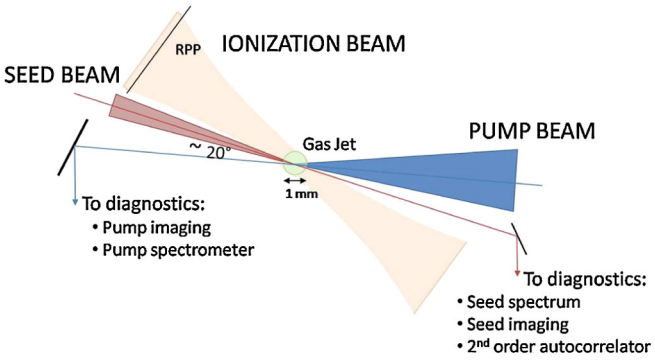

FIG. 1 (color online). Experimental scheme showing the three laser beams focused at the center of a supersonic gas jet: the 3.5 ps pump beam, the quasicounter propagating 400 fs seed beam, and the 400 ps ionization beam that arrives 1 ns before the pump and seed beams to create the plasma.

beams were focused at the center of a supersonic high pressure gas jet.

The ionization beam was smoothed with a random phase plate (RPP), leading to an intensity of $3 \times 10^{13}\,\mathrm{W/cm^2}$. It ionized a volume of 1.4 mm (in the pump-seed propagation direction, horizontal plane) by 0.24 mm (transverse direction, vertical plane) of a gas jet produced by a 1 mm diameter nozzle. The plasma is created by multiphoton ionization of the gas followed by avalanche ionization in electron-atom collisions [9]. The ionization state and the plasma density were controlled by adjusting the ionization beam intensity and the back pressure of the gas jet. We measured, using Thomson scattering and interferometry [8], the electron density and the average charge number that ranged from $\langle Z \rangle = 3 - 5$ for N_2 and Ar plasmas. Using our gas jet nozzle, these gases had to be used compared to lighter ones (e.g., He or H) in order to achieve the high electron densities required to enter the strong-coupling regime. The ionization of the gas produces an electron density profile which has a constant value over 600 μm within the jet. This value can be adjusted by varying the pressure of the gas. The plasma temperature has been estimated using a one-dimensional radiative hydrodynamic code [10]. For the interested electron densities, $n_e = 0.05 - 0.3 n_c$, the temperature ranges from 200 to 500 eV. The timing of the pulses was adjusted so that the ionization pulse arrived at the gas jet center 1ns before the pump and seed pulses.

The pump pulse was compressed to a pulse duration of 3.5 ps and then focused ($f/7$) to $d_p \simeq 30\,\mu$m (FWHM), leading to a maximum intensity of $I_p \sim 6.5 \times 10^{16}\,\mathrm{W/cm^2}$. At the exit of the interaction region, the beam was collected by an $f/5$ lens and sent to diagnostics (see Fig. 1). The seed pulse was compressed to the minimum duration of $t_{\mathrm{seed}} = 400$ fs, and focused ($f/6$) to $d_s \simeq 20\,\mu$m (FWHM), leading to an intensity of $\sim 5 \times 10^{15}\,\mathrm{W/cm^2}$ (as measured using the focal-spot image). At the exit of the interaction region, the beam was collected by an $f/6$ lens and sent to diagnostics. The two interacting pulses were crossed with an angle of $\alpha = 160°$ between them as shown in Fig. 1. The interaction length in the plasma is $l_{\mathrm{int}} = d_p/\sin\alpha \simeq 100\,\mu$m.

The seed pulse leaving the plasma (with or without the presence of the pump pulse) was sent to three diagnostics: i) an absolutely calibrated 2D imaging diagnostic of the focal spot, ii) an optical spectrometer for spectral analysis, and iii) a second order autocorrelator for pulse duration control. The imaging diagnostic gave us information on the absolute transmitted amplified energy, on the spatial distribution of the transmitted beam, and allowed us to check (by performing shots without seed) a possible contribution from backscattered pump light. The spectral measurements gave us the frequency distribution of the transmitted amplified seed pulse and provided as well a measure of the amplification of the signal, i.e., the energy gain. Correlation between this measurement and the 2D imaging diagnostic ensured that it was not sensitive to spatial filtering induced by the entrance slit of the spectrometer. The autocorrelator was used to discern between the longer backscattered pump light, originating from thermal noise induced by SRS and SBS, and the shorter seed signal. Correlation between these three diagnostics allowed us to distinguish experimental artefacts from an effective seed beam amplification.

Figure 2(a) shows signals recorded on the seed spectral diagnostic. The reference spectrum, I_{s0}, represents the seed at the exit of the plasma without pump. The pump SBS backscattered light spectrum, $I_{p\text{-BS}}$, collected by the seed optics in the absence of the seed, is also shown. This is found to be small, consistent with the PIC simulations that were run using our experimental parameters. Finally, the transmitted seed when the pump is on, I_s, is displayed, both with the pump and seed polarizations parallel or crossed. The beam geometry and plasma conditions are the same for the four cases. A 35-fold (I_s/I_{s0}) enhancement of the transmitted seed is obtained only for the case of seed and pump interacting with parallel polarizations, indicating that the phenomenon of amplification is only supported by an electromagnetic coupling. Notably, the case with 90° between the two beams polarizations displays no amplification as its signal is of the same order of the pump backscattered signal. This demonstrates that the enhanced transmission (recorded when polarizations are parallel) cannot be attributed to refraction effects as potential pump beam-induced plasma perturbations would be the same in the two cases. Regardless, the amount of pump backscattered light is negligible with respect to the amplified seed signal. Taking account of the (negligible) pump backscattered light would give a relative amplification factor $R = (I_s - I_{p\text{-BS}})/I_{s0} \approx 32$, hardly different from the factor 35 shown in Fig. 2. Results similar to those

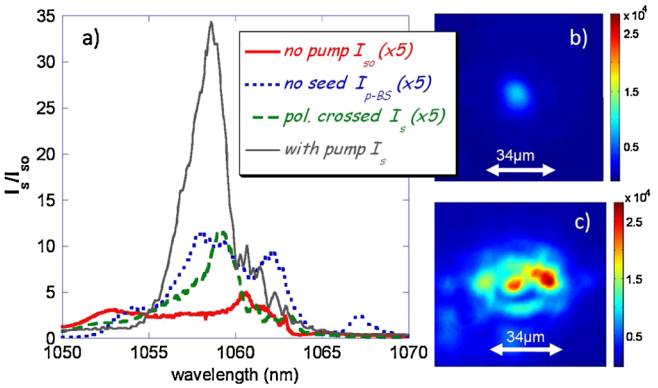

FIG. 2 (color online). (a) Transmitted signal recorded on the seed spectrometer, at the exit of an Ar plasma with density $n_e = 0.1 n_c$. Except for the amplified signal, I_s, all spectra have been multiplied by a factor of 5 for visibility. The focal spot of the seed signal transmitted through the plasma without (b) and with (c) the pump beam. Images are displayed with the same color scale.

displayed in Fig. 2(a) were obtained for every set of physical (gas, pressure, nozzle) conditions.

The duration of the amplified seed pulse, measured with the autocorrelator, is of the same order of the incident pulse. We checked that, as expected, the amplified spectrum has a FWHM in frequency of the order of the theoretically predicted $\mathrm{Im}\omega_{sc}$, where ω_{sc} is the complex frequency of the plasma quasimode [6]. The spatial profile of the amplified beam is, however, broadened and fragmented which can be attributed to pump laser beam modulations. The PIC simulations show that the pump beam is affected by filamentation and thermal SBS approximately on the same time scale. The use of a shorter seed pulse might allow the amplification process to take place in the undisturbed front part of the pump beam, and thereby avoiding the fragmentation of the amplified seed beam profile. Note that the analysis of the PIC simulated frequency spectrum of the amplified seed (not shown) confirms that the 3-wave coupling process is due to the SBS-sc.

Figure 3 shows that for a $n_e = 0.1n_c$ Ar plasma when varying the delay Δt between the pump and seed beams, the relative amplification R is observed to peak at $\Delta t = 0$.

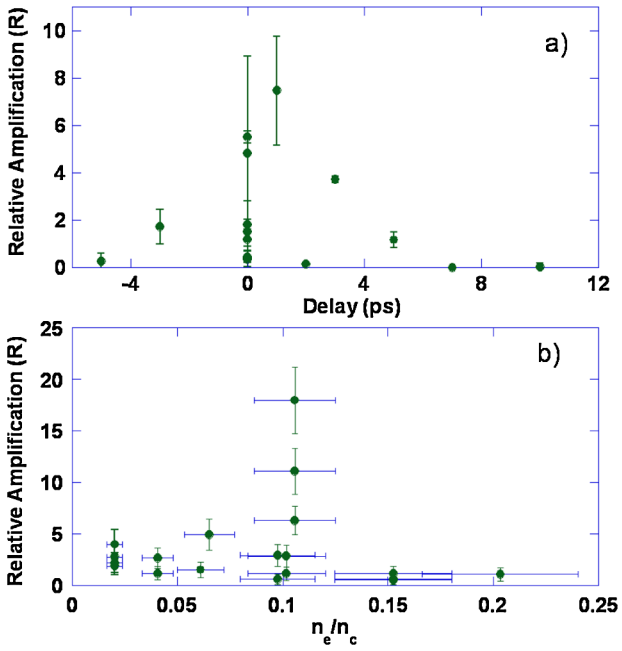

FIG. 3 (color online). (a) Relative amplification factor (R) of the seed pulse versus the time delay (Δt) between the seed and the pump pulses for an Argon plasma at $0.1\mathrm{n_c}$. (b) Relative amplification factor (R) versus plasma density in an Argon plasma at $\Delta t = 0$. Results are obtained from the spectrum of the signal and the time-integrated focal-spot image and the variation in the measurements between the two diagnostics are reflected in the error bars on R. Error bars on the density take into account the measurement uncertainty, as well as the simultaneous presence of different ionization states in the gas. The maximum amplification is different due to the fact that the two graphs correspond to two independent series of shots.

Out of these conditions, strong amplification was never obtained despite repeating the shots. The large fluctuations in amplification occurring for the best conditions are due to the reproducibility of high density plasma formation, the laser focal spots intensity fluctuations, and the beam alignment from shot to shot. Similar results are obtained for N_2.

The lower relative amplification at plasma densities below $0.1n_c$ is due to a combination of enhanced seed transmission and lowered SBS gain with decreasing plasma density. At those densities, the growth time ($t_{sc} \propto n_e^{-1/3}$) [6] becomes larger than the seed pulse duration, and the energy coupling is less efficient. The decrease of amplification for densities higher than $0.1n_c$ is correlated with the decreased transmission level of the two pulses through the plasma, in other words, a lower pump intensity yields a lower gain for sc-SBS [6]. We attribute this decreased transmission to scattering on the density fluctuations inside the plasma induced by the ionization beam. Indeed, the beamlets within the RPP smoothed ionization beam drive density perturbations, with the main ion wave having a wavelength of $\sim 14\,\mu$m. For a characteristic ion acoustic velocity of $0.1\,\mu\mathrm{m/ps}$, i.e., $T_e \approx 200\,\mathrm{eV}$, this produces a period of the order of 140 ps. Such perturbations that drive filamentation will damp out in $1 - 2$ ns. In our setup, the ionization beam irradiates the gas jet 1 ns before the pump and seed beams, i.e., before complete damping of the fluctuations. The plasma therefore still exhibits density fluctuations, random in space, at the time of the pump-seed interaction. In particular, their effect on the propagating seed beam is an enhancement of refraction of the beam, leading to i) less pump energy transferred to the seed, ii) a larger opening angle of the transmitted seed, both leading to less energy reaching the collecting lens of the diagnostics. Nevertheless, the axis of the seed beam is not changed [11]. Collisional absorption and SRS are found to be negligible. Our PIC simulations show that with densities below the quarter-critical density, the SRS excitation is limited to the first $1 - 2$ps and amounts to a maximum of 3–4% of pump energy averaged over the whole pulse temporal length.

We find that the measured acquired energy by the seed is consistent with full pump depletion. One can estimate the energy acquired by the seed at the exit of the interaction region as a function of the pump energy $\Delta E_{\mathrm{seed}} = FE_{\mathrm{pump}}$, where the factor F takes into account the geometrical and temporal overlap between the two Gaussian beams and the measured seed and pump transmission levels. For example, for Ar at $0.1n_c$, F was calculated to be $\simeq 0.002$ which means 4 mJ acquired from a 2 J pump. This compares well with 5 mJ measured experimentally.

The absolute amplification (I_s/I_v, where I_v is given by the seed transmitted energy in vacuum) reaches at low densities (e.g., at $0.02n_c$ for N_2 corresponding to little attenuation for the seed) a maximum of 4, corresponding to a maximum amplified energy of 60 mJ. At higher densities, this factor drops below 1 and the parameter of

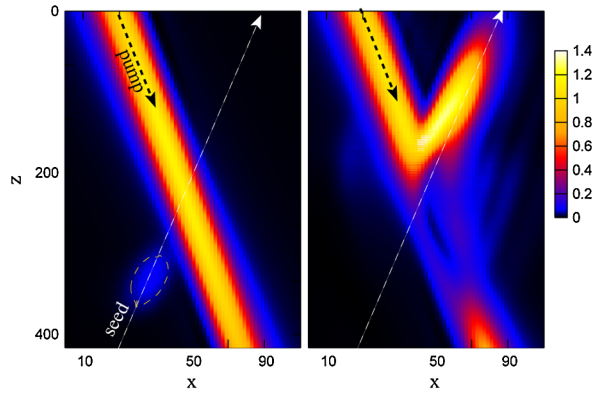

FIG. 4 (color online). Simulation results showing the electromagnetic field intensity, normalized to the incident pump intensity at focus, before (left) and after (right) the seed interaction with the pump. Spatial dimensions are in μm.

interest is the relative amplification factor $R = (I_s - I_{p\text{-BS}})/I_{s0}$, independent of attenuation.

Accompanying simulation results are obtained with the nonparaxial wave-coupling code KOLIBRI [12]. It is based on a two-dimensional nonlinear fluid description of the plasma and solves the electromagnetic wave equation. A recent version of the code allows for inhomogeneous density profiles, which has been used in order to take into account plasma density profiles closer to the experimental conditions. Losses due to inverse bremsstrahlung are also included in the code. In the simulation, a seed pulse with the intensity of 5×10^{15} W/cm^2 and 400 fs duration (at FWHM) crosses, with an angle of 163°, the pump pulse having a temporally constant intensity 6.5×10^{16} W/cm^2 over the considered time window (2 ps). The plasma density plateau was set to $0.1n_c$ and temperatures to $T_e = 500$ eV and $ZT_e/T_i > 10$. The mass number is $A = 40$ (Ar) and the average ionization is $Z = 5$. It can be seen in Fig. 4 that i) the peak intensity of the seed pulse is amplified by a factor ~15–20 and ii) the pump pulse is depleted in and behind the region where the seed pulse has crossed the axis of the pump. The simulation is thus well consistent with the experimental observations. We checked that Landau damping of the excited ion waves as well as density profile modifications due to the strength of the pump do not affect the seed pulse amplification in the considered time window.

The simulation with the fluid plasma model confirms the kinetic PIC simulations [3,6]. Both kinetic and fluid simulations that are run here show excitation of a large-amplitude ion-acoustic wave that plays the role of a Bragg-grating that reflects the pump beam in a direction slightly different from that of the seed. This, in addition to the autocorrelator diagnostic measuring, the duration of the amplified seed pulse allows us to distinguish between the amplified seed and the redirected pump.

Ion kinetic effects, such as ion trapping and ion wave breaking [7], will eventually limit the possible seed amplification. These effects result in $t_{sc} \leq t_{\text{seed}} \leq t_{wb}$, where $t_{wb} = \sqrt{2m_i/m_e}/2k_o v_{osc}$ is the characteristic time scale for ion wave breaking in the sc regime. This provides a theoretical limit for the amplitude of the amplified signal: $t_{sc} \sim t_{wb}$, which gives: $a_{\max} \sim (m_i/Zm_e)^{1/2} n_e/n_c$, where $a = v_{osc}/c$ is the dimensionless electric field amplitude. In a $n_e = 0.1n_c$ plasma, one can expect to achieve $a_{\max} \sim 3$ which corresponds to intensities of the order of a few times 10^{19} W/cm^2.

This first experiment, even in not optimal conditions, was intended as a proof-of-principle demonstration of sc-SBS amplification. There are several paths of improvement: reducing density inhomogeneities in the plasma that would allow a better propagation of the pulses and a reduction of the attenuation. With an homogeneous plasma, transition to higher plasma densities above $0.25n_c$, while keeping low attenuation, would improve the overall interaction conditions and the maximum amplification factor, as shown in PIC simulations. Also, for future experiments, the effective interaction length could be increased by using a multistage configuration.

The authors are thankful to Dr V. Lisitsa and Dr. V. Krainov for constructive suggestions on the ionization physics and to Dr. A. A. Andreev for helpful discussions. We acknowledge the financial support from Grant No. E1127 Région Ile-de-France and the *Agence Nationale de la Recherche* under Project No. ANR-07-BLAN-004. M. N. was supported by JSPS. The numerical simulations were performed on the computing centers *CCRT* of the CEA and *IDRIS* of the CNRS.

*Corresponding author: julien.fuchs@polytechnique.fr

[1] M. Maier *et al.*, Phys. Rev. Lett. **17**, 1275 (1966).
[2] R. D. Milroy *et al.*, Plasma Phys. **19**, 989 (1977); Phys. Fluids **22**, 1922 (1979); A. A. Andreev and A. N. Sutyagin, Sov. J. Quantum Electron. **19**, 1579 (1989).
[3] Z.-M. Sheng *et al.*, Appl. Phys. B **77**, 673 (2003).
[4] V. M. Malkin *et al.*, Phys. Rev. Lett. **82**, 4448 (1999);Phys. Rev. Lett. **84**, 1208 (2000);B. Ersfeld and D. A. Jaroszynski, Phys. Rev. Lett. **95**, 165002 (2005).
[5] C.-H. Pai *et al.*, Phys. Rev. Lett. **101**, 065005 (2008); R. K. Kirkwood *et al.*, Phys. Plasmas**14**, 113109 (2007); J. Ren *et al.*, Nature Phys. **3**, 732 (2007); W. Cheng *et al.*, Phys. Rev. Lett. **94**, 045003 (2005).
[6] A. A. Andreev *et al.*, Phys. Plasmas **13**, 053110 (2006).
[7] D. Forslund *et al.*, Phys. Fluids **18**, 1002 (1975).
[8] L. Lancia *et al.*, Proc. SPIE **7359**, 7359ON (2009).
[9] J. Denavit *et al.*, Phys. Plasmas **1**, 1971 (1994).
[10] J.-R. Marquès, Ph.D. thesis, Université de Paris Sud, Orsay (1992).
[11] M. Grech *et al.*, Phys. Rev. Lett. **102**, 155001 (2009).
[12] S. Hüller *et al.*, Phys. Scr. **T63**, 151 (1996); Phys. Plasmas **4**, 2670 (1997).